The Effect of Dynamic Synapses on Spatio-temporal Receptive Fields in Visual Cortex

Ömer B. Artun, Harel Z. Shouval and Leon N Cooper

Departments of Physics and Neuroscience

and

Institute for Brain and Neural Systems

Brown University

Providence RI 02912

December 8, 1997

Technical Report No.78

Abstract

Temporal dynamics are a well known feature of synaptic transmission [1]. Recently [2, 3] temporal dynamics of synaptic transmission has been reported in neocortex. Here we examine the possible effects of these dynamics on the spatio-temporal receptive fields of simple cells in V1. We do this by examining a simple model [4] of a cortical neuron that depends on an oriented thalamocortical projection. In our model, the receptive field (RF) structure is encoded either as a structured presynaptic probability of release or as a structured postsynaptic efficacy. We show that these different assumptions about the origin of receptive field structure lead to very different spatio-temporal dynamics. The structured efficacy model (SE) leads to tuning curves that are unimodal, and although the response magnitude changes in time, the preferred orientation does not. On the other hand, the structured probability model (PR) leads to tuning curves which are not unimodal and change their preferred orientation in time. We show that the temporal code induced by the dynamic synapses can be used for distinguishing between different input that induce the same average firing rate.

Temporal dynamics are a feature of all synapses [1], however the functional consequences of such dynamics are not clear. Recent work has revealed novel aspects of the temporal dynamics of synaptic transmission in neocortex [2, 3]. The major findings reveal short term depression in both cortico-cortical [2, 3] and thalamocotical synapses [5, 6], where the rate of the depression in thalamocortical synapses seems to be larger than in cortico-cortical synapses. The depression is frequency dependent; the steady-state magnitude of the EPSC is approximately inversely proportional to the frequency of stimulation ($\approx 1/\mu$) [7, 3]. Further, it has been found [2] that potentiation enhances the depression. Thus causing 'potentiated' synapses to be potentiated only in response to the first spikes in a moderate (5-50 Hz) frequency range and actually depressed for the rest of the pulses. The properties of these synapses have implications on spatio-temporal properties of cortical RF's and on how established cortical plasticity mechanisms affect the formation of cortical RF's. In this paper, we investigate the effect such synapses have on a model of simple, single cell exhibiting orientation selectivity. We assume that the dynamical of properties of synapses that were investigated in vitro are not significantly altered in vivo [8]. Real cortical cells interact with neighboring cells, these interactions may effect their properties, however it has been shown [4] that non-interacting cells already show orientation selectivity similar to those observed in interacting cortical cells. Furthermore, most models invoking cortical interactions in order to sharpen orientation selectivity require a seed of orientation selectivity at the thalamocortical level [9, 10].

The properties of cortical receptive fields are experience dependent [For example see review by Katz and Shatz 1996] , and the most likely candidates for the cellular mechanism that underly this plasticity are Long Term Potentiation (LTP) and Long Term Depression (LTD). There is a long standing debate concerning the nature of this change. One view is that LTP changes the presynaptic probability of release [12, 2]. Another view is that synaptic efficacy is changed [13, 14, 15]. If probability of release is altered by LTP, cortical receptive fields may be composed of a structured probability of release, whereas if efficacy is altered by LTP, receptive fields may be composed of a structured efficacy. In this paper we examine the effects of these, two different, possibilities on the spatio-temporal structure of receptive fields in visual cortex.

The model we propose is composed of several components, temporal dynamics of synaptic conductance, assumptions about receptive field structure and assumptions about the input. The equations of synaptic dynamics used are similar to the ones described as in [7]. The amount of available neurotransmitter resources (R) that can be released to the synaptic cleft is governed by

$$\frac{dR}{dt} = -p_r \sum_i \delta(t - t_i^{AP})R + \frac{1-R}{\tau_r} \tag{1}$$

where $t = t_i^{AP}$ are the arrival times of action potentials and $\tau_r \approx 600msec$ [1] is the re-uptake time constant. The postsynaptic conductance (G) is governed by

$$\frac{dG}{dt} = -\frac{G}{\tau_i} + \sum_i e\, p_r\, R\, \delta(t - t_i^{AP}) \tag{2}$$

where τ_i ($\approx 1 - 2$ ms) is the inactivation time constant of transmitter gated ion channels and e is the postsynaptic efficacy. The voltage response of the postsynaptic cell is modeled as a leaky integrate-and-fire neuron[2].

$$\tau_{mem}\dot{V} = -(V - V_{rest}) - R_l \sum_{k,synapses} (V - E_s)G_k \tag{3}$$

The model we assume for retinal preprocessing, LGN and cortical receptive fields are shown in figure (1). The cortical receptive fields can be formed by spatial modulation of one or both of the parameters in the synaptic dynamics, namely *synaptic efficacy* or *probability of release*. We examine two extreme cases as to the cellular origin of thalamocortical structure.

- *Case 1:* **Probability of release (PR) Model:** We assume the $e(\vec{r})$ is constant for both ON/OFF channels, $p_r(\vec{r})$ is spatially modulated to form the RF.
- *Case 2:* **Synaptic efficacy (SE) Model:** We assume $p_r(\vec{r})$ is constant for both channels and $e(\vec{r})$ is spatially modulated to form the RF.

[1] Approximately the time identified by experiments *in vitro*

[2] The parameters used are $\tau_{mem} = 50$ $msec$, equilibrium potential $E_s = 0$ and resting potential $V_{rest} = -65mV$.

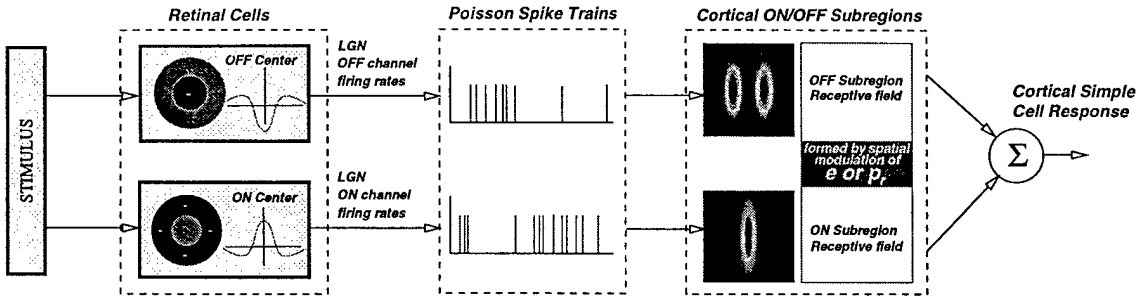

Figure 1: Retinal cells have ON/OFF center surround receptive fields. LGN cells produce spike trains with Poisson statistics with rates set by the luminance of the visual stimulus after center surround filtering. The center surround receptive fields is realized through difference-of-gaussians (DOG) filter. The stimulus (16x16 patch) is preprocessed with ON/OFF center ($\sigma_+ = 1, \sigma_- = 3$ for ON center, reverse for OFF center) DOG filter to yield the firing rates of LGN cells. The cortical simple cell receives afferent synaptic inputs LGN cells with temporal dynamics described in text. The cortical receptive fields for ON/OFF subregions are formed by spatial modulation of efficacy or probability of release. Thalamic inputs have a spontaneous activity level of 15 Hz. Before stimulus presentation, LGN cells have been excited with spontaneous activity for 400 ms. in order to stabilize synaptic conductance. We have examined two types of inputs, flashed bars which are presented for 300 ms, and drifting sinusoidal gratings for 1600 ms. The temporal and spatial frequency of the gratings were $\omega = 2Hz, \lambda = 5pixels$, respectively. Changing contrast corresponds to modulating the maximum value of the average firing rate above spontaneous activity.

Responses of cells to **flashed bars** can reveal more aspects of the temporal dynamics of synaptic conductance. Orientation tuning curves[3] as shown in figure (2) are trial averages of the responses over different time scales. At the onset of the stimulus a rapid increase in the firing rate is followed by a decrease due to synaptic depression. The PR model shows changing orientation selectivity in time. At non-preferred orientations the increase in the firing rate at the onset of the stimulus is small but sustained firing rates are higher than for the preferred orientation. The SE model however, shows consistent selectivity in time due to the fact that the effect of depression is constant regardless of orientation. We can use a simplified version of the model to analytically derive similar results. We assume that a flashed bar has two regions, high and low, and the regulation of probability of release has two values, high and low, thus there are effectively four types of synapses that contribute to the conductance of the neuron. Analysis of this simplified system is given in Appendix A. The reason for the different temporal dynamics, of these models, is that synaptic depression is enhanced by high P_r and by presynaptic firing rate. In the PR model both of these

[3]An interactive demo program (written with Matlab 5 for unix platforms) can be obtained from `http://www.physics.brown.edu/people/artun/publications/`. This program contains all source code for interactively generating tuning curves for flashed bars.

factors are compounded. Thus, when a bar at an optimal orientation is presented, synapses excited by that bar would depress faster in the PR model than in the SE model.

What purpose could temporal dynamics serve? To investigate this problem, we used a simpler model without employing ON/OFF channels. The cortical receptive field assumed is a Gaussian strip oriented along the preferred direction. It is possible to obtain the same average firing rates for stimuli, that differ in several of their properties, for example orientation and contrast. A single neuron, employing a firing rate code, could not be used to distinguish between such stimuli. However it is possible that the temporal dynamics of the conductance, brought about by the synaptic dynamics, could produce a temporal code that can be used to distinguish between these inputs.

In figure (3) an example of this is given, for two different inputs, which yield same mean firing rate over a 300 ms period. However over the first $60ms$ the firing rate in the high contrast non preferred orientation is higher (581 ± 62 spikes) than for the other input (469 ± 76 spikes), whereas over the next 60 ms this is reversed and the conductance take the values (308 ± 49 spikes) and (344 ± 52 spikes) respectively. This type of a, two dimensional temporal, code arises from the dynamics of the synapses and can help distinguish between the different inputs, furthermore, it may actually contribute to temporal codes observed in cortex [16]. **Drifting sinusoidal gratings** are swept across the visual environment. The magnitude of the F1[4] component of the conductance is computed for both models. The results for both models (figure(4)) reveal plausible tuning curves (even though there is a slight increase in the tail of tuning curve for PR model). To explain the difference from flashed bar results qualitatively, it is simpler to examine the situation where the gratings are rectangular rather than sinusoidal. At 2 Hz stimulation the synapses will have time (500 ms) to recover, before they experience a change in stimulus frequency, thus each onset of stimulation will produce an increase in conductance. We simulated and analyzed the effect of dynamic synapses on two simple models of orientation selectivity in simple cells in V1. Receptive fields composed of a synaptic efficacy structure show properties similar to those displayed by cortical receptive fields [for

[4]F1 is the sweeping frequency, the conductance $G(t)$ is Fourier transformed $\tilde{G}(\omega)$ and magnitude is calculated for this frequency.

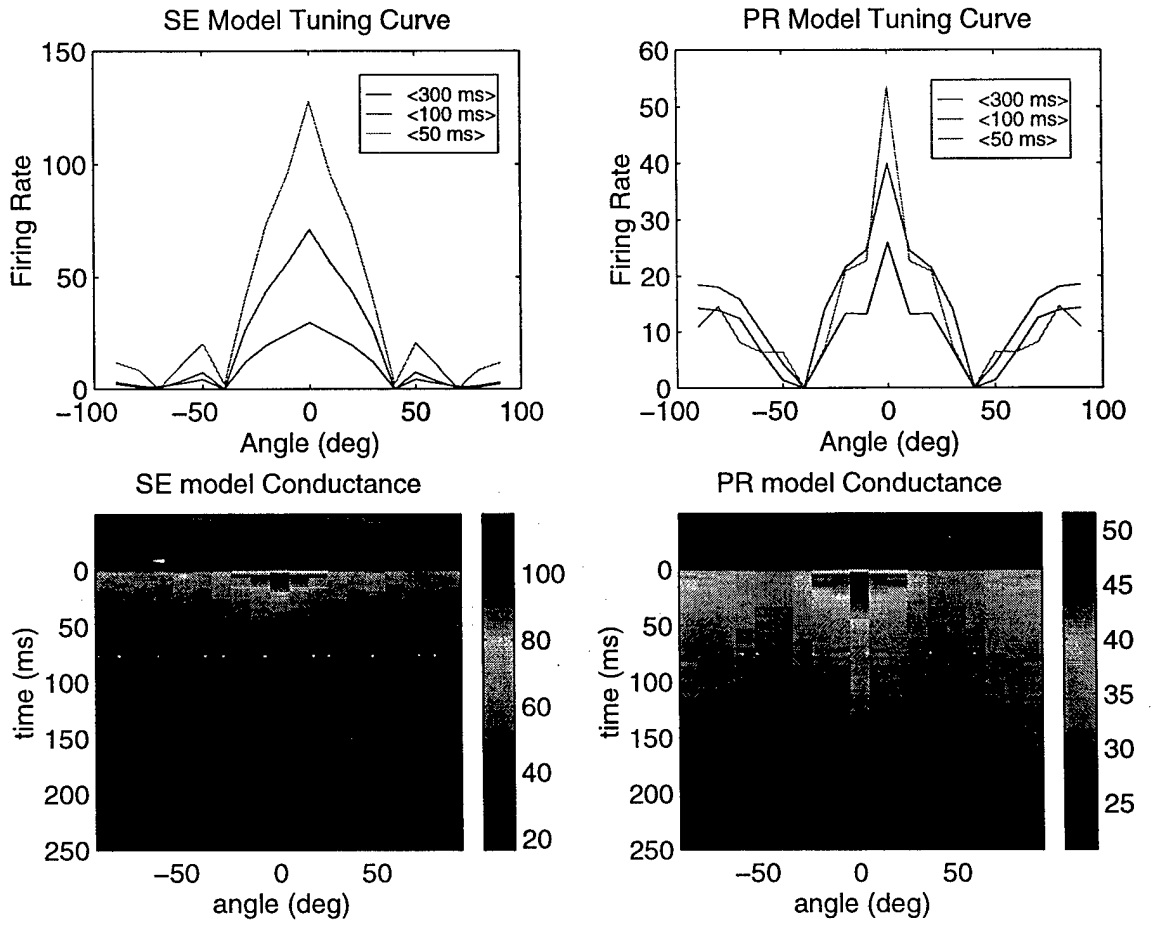

Figure 2: **A, B** Tuning curves for SE and PR model respectively. Firing rates are averaged over 50, 100, 300 ms for both models. The SE model shows unimodal tuning curves at all times whereas PR model shows bimodal tuning curves in which the angle that produces maximal response changes over time. **C,D** color coded representations of averaged conductances as a function of time and angle. After the stimulus is presented there is a rapid onset of activity, which decays in time due to synaptic depression. In the SE model, activity decays equally for all orientations whereas in the PR model activity decays faster in the preferred orientation thus causing the sustained activity in the preferred orientation to be lower than in the orthogonal direction.

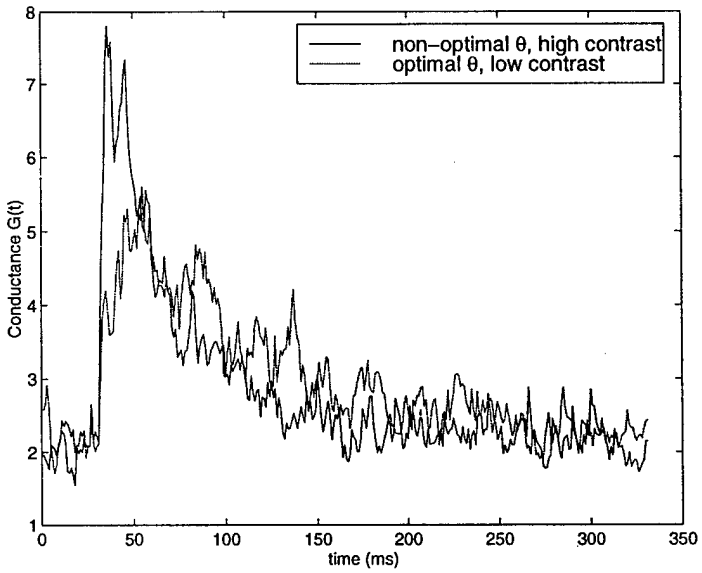

Figure 3: Bars at high contrast (presynaptic rate 60 Hz), , non optimal orientation ($\theta = 40$ deg), and low contrast (presynaptic rate 20 Hz) optimal orientation ($\theta = 0$ deg) are presented. Both stimuli produce the same mean conductance rate 300 ms, however the temporal time course is clearly different.

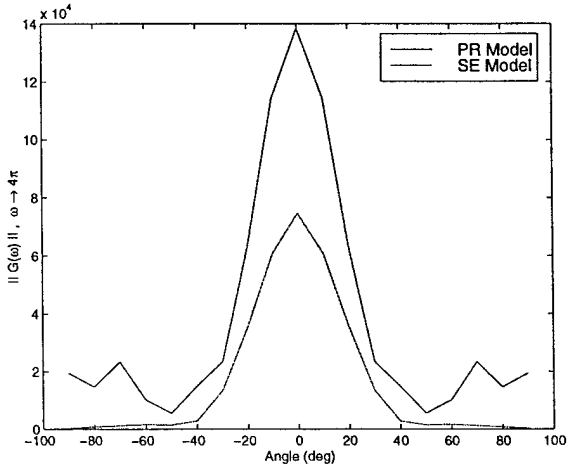

Figure 4: Orientation tuning curves for 2 Hz. stimulation. tuning curves are generated by calculating the magnitude of stimulation frequency component of the Fourier transform.

review see Orban, 1984]. The orientation tuning curve is unimodal and retains the same prefered orientation over time. Increasing the contrast, causes an increase in firing rates at low contrasts and tends to saturate at high contrasts. For flashed bars we can see that the response has a quick transient peak, the magnitude and slope of the peak increases with the contrast of the stimuli. This peak then decays, it decay faster for high contrast stimuli than for low contrast stimuli. The firing rate decay in our model is indicative of the synaptic dynamics, and depends on the parameters of synapses such as their recovery time. This also resembles the behavior of cortical neurons although in cortical neurons the decay of the response can depend on other factors as well, such as depression of LGN responses for prolonged inputs and on network effects. In contrast, the structured p_r model has bimodal tuning curves that change their orientation in time. We have not found evidence in the literature that such cells exist. [5] It is possible, however, that models in which both p_r and e have spatial structure would exhibit biologically plausible tuning curves.

Abbott and his co workers [3] have suggested that the purpose of the synaptic depression is to make synaptic conductances sensitive to changes in firing rates, rather than to their magnitude. Coupling this property with a spatial receptive field structure, produces cells with a spatio-temporal receptive field that encode 'features' as well as changes in those features, such as contrast changes. We have shown evidence that the temporal structure of the response can be used to distinguish between features that can not be distinguished by firing rate alone. Qualitatively similar results have been obtained experimentally [16] and have been shown to enhance the capacity of the neural code [20].

Appendix A

For the flashed-bar stimulus the steady state behavior of the PR model can be calculated. From the governing equations for a fixed rate μ the asymptotic behavior of the resources (R) can be written

[5] Studies which have used reverse correlation techniques have found receptive field **kernels** that change in time [18, 19], however the results of such experiments can not be compared to the results shown here because of the difference between the reverse correlation methods, used in those experiments, and the flashed bar input, which we simulated.

as

$$R(\infty) = 1/(1 + \mu p_r \tau_r). \tag{4}$$

The same can be done for the conductance that leads to

$$G(\infty, \vec{r}) = \tau_i e(\vec{r}) p_r(\vec{r}) \mu \frac{1}{1 + p_r(\vec{r})\mu\tau_r} \tag{5}$$

The conductance of the postsynaptic cell is defined as $G_T(\infty) = \int_S G(\infty, \vec{r}) d\vec{r}$. To explain the behavior of the PR model, we can think of the experiment in the simplest case of two overlapping bars which have an angle θ between them. The LGN activity has a high firing rate along the bar and low firing rate elsewhere (μ_l, μ_h), similarly the receptive field is formed from a high probability of release along the bar and low probability of release elsewhere (p_{rl}, p_{rh}). We can approximate the integral to a sum of 4 components weighed by the area. We can identify 4 distinctive regions $((p_{rl}, \mu_l), (p_{rl}, \mu_h), (p_{rh}, \mu_l), (p_{rh}, \mu_h))$, with corresponding areas A_1, A_2, A_3, A_4. The areas can be approximated by a receptive field and an input composed of a rectangular bar of length a width b, and the angle between them is θ. For $\theta > \arctan a/b$ we can approximate areas by,

$$A_1 = a^2 / \sin\theta \tag{6}$$

$$A_2 = A_3 = ab - a^2 / \sin\theta \tag{7}$$

$$A_4 = \pi b^2/4 - 2ab + a^2 / \sin\theta \tag{8}$$

The total conductance can be written as

$$G_T(\infty) = \tau_i e\left(\frac{A_1 p_{rl}\mu_l}{1 + p_{rl}\mu_l\tau_r} + \frac{A_2 p_{rl}\mu_h}{1 + p_{rl}\mu_h\tau_r} + \frac{A_3 p_{rh}\mu_l}{1 + p_{rh}\mu_l\tau_r} + \frac{A_4 p_{rh}\mu_h}{1 + p_{rh}\mu_h\tau_r}\right) \tag{9}$$

To obtain a bell shaped tuning curve the quantity $\partial G_T/\partial\theta$ has to be negative for $\theta > 0$ (and positive for $\theta < 0$). For a typical parameter regime, we see that the sign of $\partial G/\partial\theta$ is always greater than

zero. Hence, we deduce that the average conductance for the PR model in the long time limit can not yield a bell shaped tuning curve.

References

[1] Zucke, R. S. In *Annual Review of Neuroscience,* Cowan, W. M., Shooter, E. M., Stevens, C. F., and Thompson, R. F., editors, volume 12, 13–32. Annual Reviews, Palo Alto, CA (1989).

[2] Markram, H. and Tsodyks, M. V. *Nature* **382**, 807–810 (1996).

[3] Abbott, L. F., Varela, J. A., Sen, K., and Nelson, S. B. *Science* , 220–223 (1997).

[4] Ferster, D., Chung, S., and Wheat, H. *Nature* **380**, 249–252 (1996).

[5] Stratford, K. J., Tarczy-Hornoch, K., Martin, K. A. C., Bannister, N. J., and Jack, J. J. B. *Nature* **382**, 258–261 (1996).

[6] Gil, Z., Amitai, Y., Castro, M. A., and Connors, B. W. *Neuron* **19(3)**, 579–586 (1996).

[7] Tsodyks, M. V. and Markram, H. *Proc. Natl. Acad. Sci.* **94**, 719–723 (1997).

[8] J., C.-A. M. and Connors, B. W. *The Journal of Neuroscience* **16(23)**, 7742–7756 (1996).

[9] Somers, D., Nelson, S. B., and Sur, M. *Journal of Neuroscience* **15**, 5448–5465 (1995).

[10] Ben-Yishai, R., Bar-Or, R. L., and Sompolinsky, H. *Proc. Natl. Acad. Sci. USA* **92**, 3844–3848 (1995).

[11] Katz, L. C. and Shatz, C. J. *Science* **274**, 1133–1138 (1996).

[12] Stevens, C. F. and Wang, Y. *Nature* **371**, 704–707 (1994).

[13] D., L., A., H. N., and R., M. *Nature* **375**, 400–404 (1995).

[14] Isaac, J. T., Nicoll, R. A., and Malenka, R. C. *Neuron* **15**, 427–434 (1995).

[15] Isaac, J. T., Crair, M. C., Nicoll, R. A., and Malenka, R. C. *Neuron* **18**, 269–280 (1997).

[16] Gawne, T. J., Kjaer, T. W., and Richmond, B. J. *Journal of Neurophysiology* **76**, 448–453 (1996).

[17] Orban., G. A. *Neuronal Operations in the Visual Cortex.* Springer Verlag, (1984).

[18] Deangeglis, G. C., Ohzawa, I., and Freeman, R. C. *Trends in Neuroscience* **18**, 451:458 (1995).

[19] Ringach, D. L., Hawken, M. J., and Shapley, R. *Nature* **387** (1997).

[20] Shouval, H. and Artun, O. B. In *to appear in proceedings of CNS*97,* (1997).

Acknowledgements

This work was supported in part by the Charles A. Dana Foundation, the Office of Naval Research and the National Science Foundation. We wish to thank Brian Blais and Barry Connors for useful discussions and technical help.